*engineering proceedings*

MDPI

*Proceeding Paper*

# Study on the Effect of Reactor Scale on Hydrogen Generation from Aluminum Alloy Powder and Water via Stirring †

**Ryoji Imai [1,*], Rina Nishiyama [2], Yusuke Yamamoto [2] and Masahiro Sakai [1,*]**

[1] Aerospace Systems Engineering Unit, Muroran Institute of Technology, Muroran 050-8585, Japan
[2] Aerospace Engineering Course, Graduated School, Muroran Institute of Technology, Muroran 050-8585, Japan
* Correspondence: r_imai@muroran-it.ac.jp (R.I.); msakai@muroran-it.ac.jp (M.S.); Tel.: +81-143-46-5356 (R.I.); +81-143-46-5377 (M.S.)
† Presented at the 4th International Electronic Conference on Processes, 20–22 October 2025; Available online: https://sciforum.net/event/ECP2025.

**Abstract**

Hydrogen is a promising $CO_2$-free energy carrier, but conventional production from fossil fuels generates $CO_2$. This study explores an alternative—reacting waste-derived aluminum alloy powder with water under stirring to generate hydrogen, combining recycling with carbon-neutral hydrogen production. In a 500 mL stirred reactor, the hydrogen yield using alloy powders was six times greater than in a 100 mL reactor, exceeding simple volume-based scaling. Excess hydrogen production is attributed to impeller-driven particle fragmentation. To quantify this, correlations between alloy mass–power input and hydrogen yield were examined, but no clear relationship was found. Future work will systematically analyze the effects of the reactor scale, stirring speed, and alloy mass on hydrogen generation.

**Keywords:** hydrogen production; reaction of water and aluminum; aluminum powder; aluminum alloy powder; stirring; scale effect

check for updates

Academic Editor: Giancarlo Cravotto

Published: 16 April 2026

**Citation:** Imai, R.; Nishiyama, R.; Yamamoto, Y.; Sakai, M. Study on the Effect of Reactor Scale on Hydrogen Generation from Aluminum Alloy Powder and Water via Stirring. *Eng. Proc.* **2025**, *117*, 74. https://doi.org/10.3390/engproc2025117074

**Copyright:** © 2026 by the authors. Licensee MDPI, Basel, Switzerland. This article is an open access article distributed under the terms and conditions of the Creative Commons Attribution (CC BY) license (https://creativecommons.org/licenses/by/4.0/).

## 1. Introduction

Hydrogen is considered a promising solution for mitigating global warming due to its potential to provide $CO_2$-free power when used in fuel cells and power generation systems [1]. Traditionally, hydrogen production relies heavily on fossil fuel reforming, which emits $CO_2$. This study investigates an alternative method of generating hydrogen by stirring aluminum alloy powder in water. The aluminum alloy powder, sourced from waste aluminum, is processed using renewable energy, thus contributing to waste recycling through carbon-neutral hydrogen production. This approach explores the feasibility of establishing a sustainable hydrogen production plant.

Chang et al. reviewed hydrogen production via electrolysis and hydrolysis, and described a method using aluminum as an example of hydrogen production through hydrolysis [2]. Aluminum reacts with water via the following reaction, producing hydrogen and aluminum hydroxide [2].

$$2Al + 6H_2O \rightarrow 2Al(OH)_3 + 3H_2 \quad (1)$$

In general, the surface of aluminum is covered by a protective oxide layer; the reaction shown in Equation (1) does not readily proceed. Wang et al. provided a review of studies on hydrogen production using aluminum and aluminum alloys [3]. In this

review, methods based on the assistance of alkalis and those under neutral conditions are introduced; however, the present study seeks approaches that do not have an adverse environmental impact, and therefore the former is not considered. On the other hand, for hydrogen production under neutral conditions without the use of alkalis, methods employing mechanical alloying—where highly surface-active alloy particles are generated through ball milling—have been investigated [4–12]. This method can achieve a high hydrogen generation rate; however, it remains questionable whether the mechanochemical alloying method using ball milling can achieve alloy production rates suitable for practical plant-scale applications. On the other hand, as catalytic approaches, the use of an M-B/$\gamma$-$Al_2O_3$ (M=Co, Ni) catalyst [13] and that of a graphite-mixed $Al(OH)_3$ catalyst [14] have been explored, both of which achieve high hydrogen production rates. However, applying the preparation and processing procedures for these catalysts to practical plants is not realistic, and the environmental impact associated with the catalysts cannot be neglected. In addition, studies have explored the utilization of the catalytic effect of aluminum hydroxide, a by-product of the hydrogen generation reaction [15,16]. However, the former requires an alkaline solution [15], whereas the latter necessitates the modification of Al powders with $TiO_2$ [16]. If aluminum–water reactions can be realized under neutral conditions without the use of catalysts or surface modification of aluminum, hydrogen production could be achieved under environmentally compatible conditions. Kanda et al. [17] and Sugioka et al. [18] demonstrated that stirring pure aluminum and aluminum alloy microparticles in pure water leads to the generation of hydrogen without catalyst and surface activation. They proposed that the mechanism of hydrogen generation involves collisions between microparticles in water induced by stirring, which partially disrupt the oxide film formed on their surfaces, thereby allowing the above hydrogen generation reaction to proceed. These results represent highly valuable findings that could accelerate progress toward the realization of hydrogen production under clean conditions. Conversely, for the prospective application of the aforementioned hydrogen production reaction to a practical plant, a comprehensive understanding of the influence of reactor scale on the hydrogen production reaction—namely, the scale effect—is indispensable. The reactor used for hydrogen production in [17] was limited to a 100 mL stainless-steel reaction vessel only, and no investigation of scale effects was conducted. On the other hand, in [18], hydrogen production experiments were carried out using 100 mL and 2000 mL reactors with 20 g and 100 g of aluminum powder, respectively; however, no discussion regarding the influence of reactor scale on the amount of hydrogen produced was provided. In addition, in the method employing the aforementioned mechanical alloying and the catalytic approaches, the influence of the reactor scale on the reaction system has not yet been examined.

The ultimate objective of the present study is to establish a hydrogen production method based on the aluminum–water reaction with stirring without catalyst and surface activation. Previous experiments using a small stirred reactor (100 mL) compared pure aluminum powder with Al-Sn alloy powders [19,20]. In these studies, the destruction of the oxide film due to the collision of the aforementioned fine particles has not been confirmed; however, it has been reported that the alloy powders produced significantly more hydrogen, likely because stirring causes particle fragmentation, increasing the powders' specific surface area and enhancing the reaction rate. Subsequently, as a preliminary investigation of the effect of the reactor scale on the hydrogen production reaction—an essential factor for assessing scalability toward industrial applications—experiments were conducted using a 100 mL reactor and a 500 mL reactor. Hydrogen generation was tested with Al-Sn alloy powders of varying compositions.

## 2. Experimental Method

In this study, hydrogen production experiments were conducted using 100 mL and 500 mL reactors to investigate the effect of the reactor scale on hydrogen generation. Regarding the reactor volume used in this study, those employed in the previous studies mentioned in Section 1 ranged from 50 to 500 mL, except for the 2000 mL reactor reported in [18]; therefore, the present sizes were selected in consideration of comparisons with the results of these previous studies. Furthermore, this study places emphasis on comparative evaluation with previous studies that neither activated the surfaces of aluminum or aluminum alloys nor employed catalysts [17–20]. In these studies, reactors with a volume of 100 mL were predominantly used; therefore, the present reactor volume was also taken into consideration.

Figure 1 shows the 100 mL (MMJ-100, OM Labotech Co., Ltd., Tochigi city, Tochigi, Japan) reactor and the experimental setup. The reactor consists of a stainless-steel cylindrical vessel with a diameter of 34 mm and a height of 141 mm, a heating element installed on the exterior of the side wall, and a stirrer. The stirrer is equipped with a blade at the tip of the shaft, which is positioned along the central axis of the cylindrical vessel and rotated by an electric motor to stir the fluid inside the vessel. The temperature inside the cylindrical vessel was maintained at a constant level by adjusting the output of the aforementioned heating element using PID control. Figure 1b illustrates the experimental setup. Hydrogen generated in the reactor was collected in a sampling cylinder, and its volume under standard conditions was calculated from the measured temperature and pressure inside the cylinder. Prior to the hydrogen production experiments, the reactor and the interior of the sampling cylinder were purged by repeatedly supplying and venting hydrogen gas. The measured parameters included the temperature and pressure inside the reactor and the temperature and pressure within the sampling cylinder.

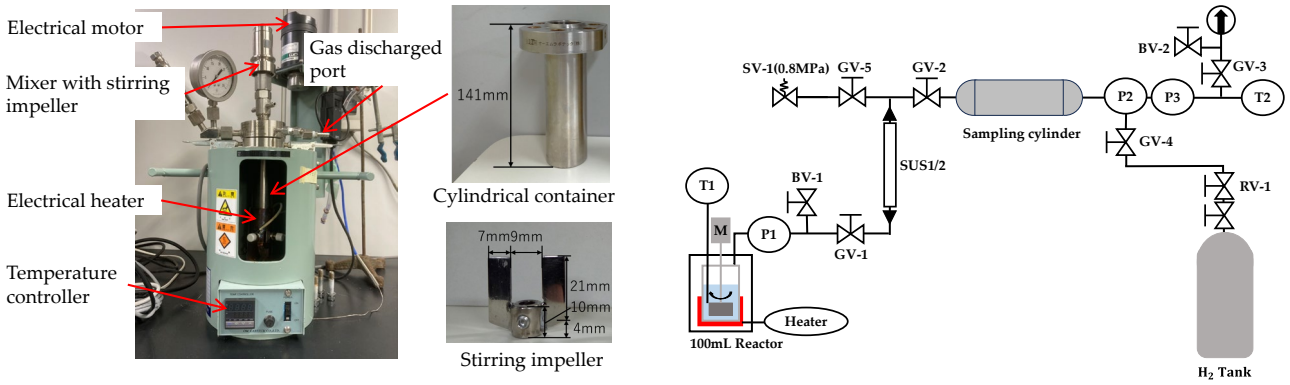


**Figure 1.** Appearance of the 100 mL reactor system and schematic diagram of the hydrogen production experimental setup (**a**) 100 mL reactor system (**b**) System schematic of hydrogen production experimental setup.

Figure 2 shows the 500 mL reactor (MMJ-500, OM Labotech Co., Ltd., Tochigi City, Tochigi, Japan) and the experimental setup. The reactor is a stainless-steel cylindrical vessel with a diameter of 50 mm and a height of 278 mm, while all other specifications are the same as those of the 100 mL reactor. The experimental setup is shown in Figure 2b; the system configuration, measured parameters, and the gas purging procedure prior to the experiments are identical to those employed for the 100 mL reactor.

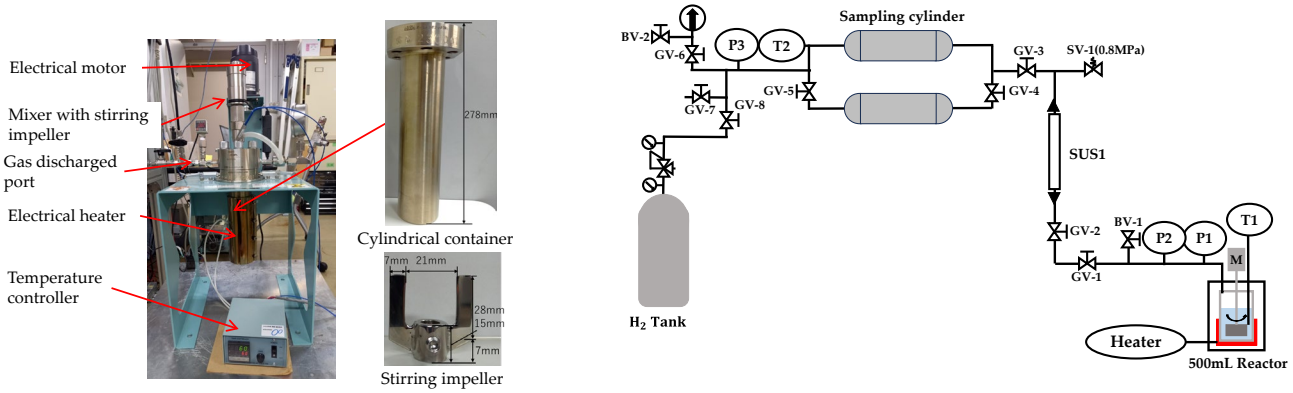


(**a**) (**b**)

**Figure 2.** Appearance of the 500 mL reactor system and schematic diagram of the hydrogen production experimental setup (**a**) 500 mL Reactor system (**b**) System schematic of hydrogen production experimental setup.

In this study, Al–50 wt% Sn and Al–5 wt% Sn powders (produced by HIKARI MATERIAL INDUSTRY Co., Ltd., Tomi City, Nagano, Japan) were used as aluminum alloy particles. These powders were produced via gas atomization. The powders were sieved using a sieve shaker (MVS-1N/1-8990-11, AS ONE Corporation, Osaka City, Osaka, Japan) to classify the particle sizes, and the particle size distributions were determined. Figure 3 shows the particle size distributions of the Al–50 wt% Sn and Al–5 wt% Sn alloy powders.

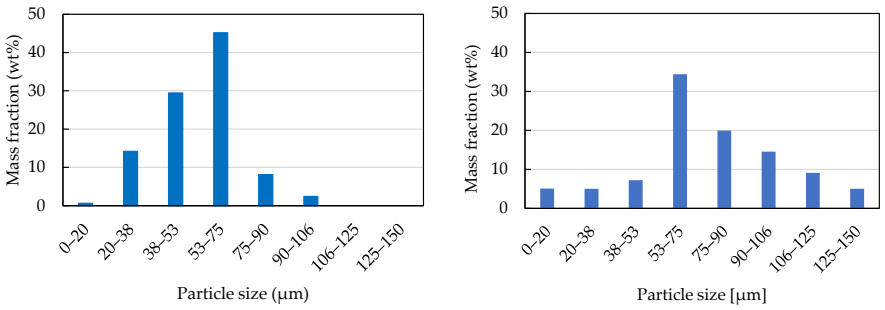


(**a**) (**b**)

**Figure 3.** Particle size distribution of alloy particles (**a**) Al–50 wt% Sn (**b**) Al–5 wt% Sn.

Table 1 summarizes the experimental conditions. A previous study [3] has investigated the relationship between the reaction temperature and the induction period, defined as the time from the start of stirring to the onset of hydrogen evolution. It was found that the induction period decreases with increasing reaction temperature and that, above 60 °C, the induction period does not shorten further. Therefore, in this study, the temperature inside the reactor was maintained at 60 °C, which corresponds to the minimum temperature at which the induction period is shortest.

**Table 1.** Experimental conditions.

| | **100 mL Reactor** | **500 mL Reactor** |
|---|---|---|
| Test liquid | Distilled water | |
| Liquid volume (mL) | 80 | 400 |

**Table 1.** *Cont.*

| | 100 mL Reactor | 500 mL Reactor |
|---|---|---|
| Temperature (°C) | 60 | |
| Composition of the particles | Al–50 wt% Sn, Al–5 wt% Sn | |
| Mass of particles (g) | 5 | 5, 25 |
| Rotational speed of stirring impellers $n$ (1/s) | 22.5 | |

## 3. Experimental Results

### 3.1. Al–50 wt% Sn Alloy Powder

Figure 4a shows the time history of hydrogen generation in the 100 mL and 500 mL reactors. The hydrogen volume is expressed at standard conditions of 20 °C and 0.103 MPa. The mass of alloy powder was 5 g for the 100 mL reactor and 5 g and 25 g for the 500 mL reactor. For the 100 mL reactor containing 5 g of alloy powder, measurements were carried out over a period of 168 h. As shown in the figure, the cumulative hydrogen production increased with time, while the rate of increase gradually declined. Notably, after 72 h, the hydrogen generation proceeded in an approximately linear manner. In previous studies [17,18], the experiments were terminated within 25 h while the hydrogen volume was still continuing to vary significantly with time. In contrast, the experimental duration in the present study is sufficiently longer than in those studies, allowing for a more rigorous evaluation of the hydrogen generation reaction. For the 500 mL reactor, two measurements were performed with 5 g of alloy powder, and the hydrogen volume at 72 h was approximately 2000 mL. In contrast, with 25 g of alloy powder, two measurements were conducted at 117 h and 168 h, and the hydrogen volume at 72 h was approximately 13,000 mL.

These results indicate that, when the mass of Al–50 wt% Sn alloy powder was maintained at 5 g, increasing the reactor volume from 100 mL to 500 mL resulted in nearly identical hydrogen production. Furthermore, when both the reactor volume and the mass of Al–50 wt% Sn alloy powder were increased five times, hydrogen production increased by approximately 6.5 times, exceeding the expected scale ratio with respect to the reactor volume and alloy powder mass.

### 3.2. Al–5 wt% Sn Alloy Powder

Figure 4b shows the time history of hydrogen generation in the 100 mL and 500 mL reactors. The mass of alloy powder was 5 g for the 100 mL reactor and 5 g and 25 g for the 500 mL reactor. For the 100 mL reactor containing 5 g of alloy powder, measurements were conducted over 168 h. As shown in the figure, the cumulative hydrogen production increased over time, while the rate of increase gradually decreased. However, after 72 h, hydrogen production proceeded in an approximately linear manner. For the 500 mL reactor, two measurements were performed with 5 g of alloy powder, and the hydrogen volume at 72 h was approximately 1100 mL. In contrast, with 25 g of alloy powder, three measurements were conducted, with hydrogen volumes at 72 h ranging from 6800 to 7900 mL. Furthermore, hydrogen production continued to increase linearly thereafter, reaching a maximum of 8400 mL at 94 h. These results indicate that, when 5 g of Al–5 wt% Sn alloy powder was used, increasing the reactor volume from 100 mL to 500 mL resulted in a decrease in hydrogen production. This finding is consistent with previous studies [8] that investigated the effect of the alloy powder concentration on hydrogen generation. Moreover, when both the reactor volume and the mass of Al–5 wt% Sn

alloy powder were increased five times, hydrogen production increased by a factor of 5–6, exceeding the expected scale ratio with respect to reactor volume and alloy powder mass. Furthermore, a comparison of hydrogen production between Al–50 wt% Sn and Al–5 wt% Sn alloy particles revealed that the Al–50 wt% Sn alloy particles produced a greater volume of hydrogen.

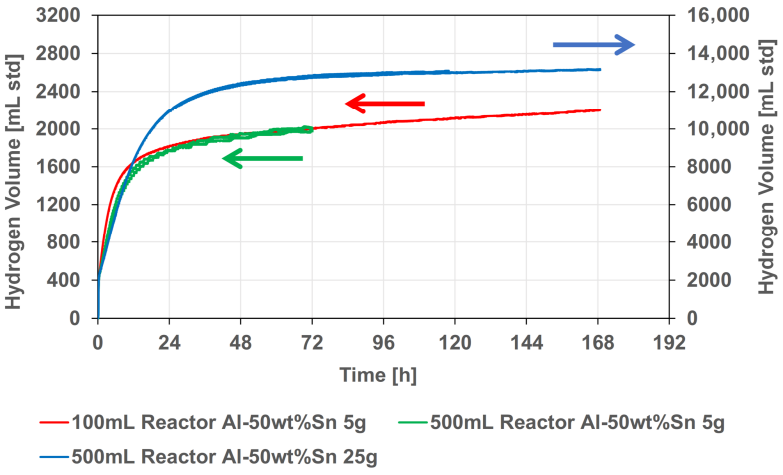


(**a**)

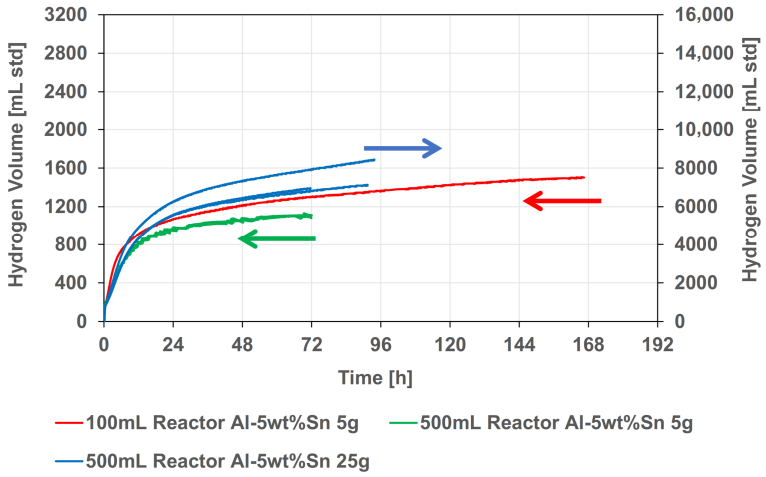


(**b**)

**Figure 4.** Time history of cumulative hydrogen production. Measurements were repeated under several experimental conditions, and all measurement results are plotted (**a**) Al–50 wt% Sn (**b**) Al–5 wt% Sn.

## 4. Characterization of Alloy Particles Before and After Experiments

### *4.1. Analytical Results of Al–50 wt% Sn Alloy Powder*

The surface condition of the alloy powders before and after the experiments was examined using a scanning electron microscope (SEM). The observation results are shown in Figure 5a. The particles exhibited an approximately spherical shape prior to the experiments, whereas many particles were observed to be non-spherical after the experiments. This is presumed to result from the fragmentation of the alloy particles due to collisions with the stirrer blades and among the particles during stirring. Furthermore, the particle surfaces exhibited irregularities, and granular aluminum hydroxide, the reaction product, was observed to adhere to the surfaces. While the deposition of reaction products on the alloy particles can inhibit the reaction, particle fragmentation leads to an increase in specific surface area, which promotes the reaction.

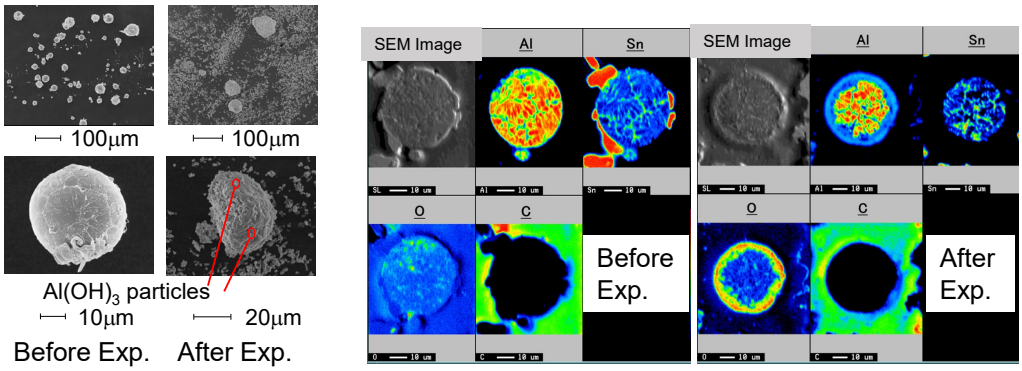


**Figure 5.** SEM and EPMA image of Al–50 wt% Sn particle. In the EPMA images, the red regions indicate high concentrations of the corresponding element, followed by green, blue, and black, in decreasing order of abundance (**a**) SEM image (**b**) EPMA image.

Next, a qualitative elemental analysis of the alloy particle cross-sections was performed using an Electron Probe Micro Analyzer (EPMA). For this analysis, the alloy particles were embedded in resin and then polished to expose the cross-sections, after which a thin layer of gold was deposited on the surface to prevent charging. Figure 5b shows the EPMA analysis results before and after the experiments. The pre-experiment analysis indicates that Sn is locally distributed on the surface of the alloy particles, while being uniformly distributed within the particle cross-sections. Such heterogeneous elemental distribution is presumed to have been formed during the alloy particle manufacturing process. A comparison of the analysis results before and after the experiments reveals that O and Al are prominently distributed on the particle surfaces after the experiments, and their presence is also observed within the particle cross-sections. The locations of these elements are considered to correspond to aluminum hydroxide, suggesting that aluminum hydroxide is present not only on the particle surfaces but also within the particles.

### *4.2. Analytical Results of Al–5 wt% Sn Alloy Powder*

Similar to the Al–50 wt% Sn alloy, the surface condition of the Al–5 wt% Sn alloy particles was observed using SEM (JCM-5000, JEOL Ltd., Akishima City, Tokyo, Japan) before and after the experiments, and an elemental analysis of the particle cross-sections was performed using EPMA (JXA-8900R, JEOL Ltd., Akishima City, Tokyo, Japan). Figure 6a shows the SEM observation results. As shown in the figure, the alloy particles exhibited an approximately spherical shape prior to the experiments. After the experiments, granular particles were observed to adhere to the particle surfaces, and non-spherical particles, presumably formed through fragmentation, were also observed. The occurrence of fragmentation is considered to be similar to that observed in the case of the Al–50 wt% Sn alloy.

The EPMA analysis (Figure 6b) revealed that, prior to the experiments, Al and Sn were uniformly distributed within the particle cross-sections. After the experiments, the proportion of Al on the particle surfaces decreased, while the distribution of O became prominent. In contrast to the Al–50 wt% Sn alloy, no distribution of O was observed beyond the near-surface region. These results indicate that, after the reaction, the reaction product—aluminum hydroxide—was present only on the particle surfaces, while no such product was detected within the particle interiors. This implies that, while the hydrogen generation reaction proceeded into the interior of the Al–50 wt% Sn particles, it occurred only at the surfaces of the Al–5 wt% Sn particles. As previously noted, this observation

is consistent with the higher hydrogen generation capacity of the Al–50 wt% Sn alloy compared with the Al–5 wt% Sn alloy.

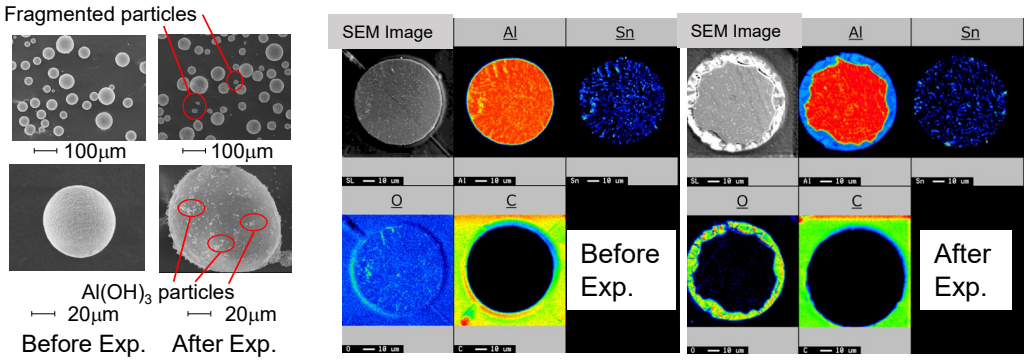


(**a**) (**b**)

**Figure 6.** SEM and EPMA images of Al–5 wt% Sn particle. In the EPMA images, the red regions indicate high concentrations of the corresponding element, followed by green, blue, and black, in decreasing order of abundance (**a**) SEM image (**b**) EPMA image.

## 5. Discussion

As described above, the hydrogen production experiments conducted in the 100 mL and 500 mL reactors revealed that the amount of hydrogen produced exceeded the scale ratio of 5.0 with respect to the reactor volume and the mass of the aluminum alloy. These findings suggest that factors other than the increased mass of the aluminum alloy contributed to the observed results. Specifically, the SEM observations of the alloy particles after the experiments revealed the presence of fragmented particles produced by stirring, indicating that the increase in specific surface area affected the reaction rate. It was further considered that the fragmentation of the particles was associated with the mechanical power imparted by stirring. Accordingly, a quantitative investigation was conducted to examine the correlation between the amount of hydrogen produced, the mass of the aluminum alloy, and the mechanical power imparted to the fluid inside the reactor by the stirring blades.

In a stirred tank, the power consumption $P$ [W] associated with the impeller is given by the power number $N_p$, which is expressed as follows.

$$P = \rho n^3 d^5 N_p \tag{2}$$

where $\rho$ denotes the liquid density [kg/m$^3$], $n$ is the impeller rotational speed [1/s], and $d$ is the impeller diameter [m]. It should be noted that the power number $N_p$ is determined by the geometry of the stirred vessel, the type of impeller, the relevant dimensional parameters, and the impeller's Reynolds number. In this study, Kamei and Hiraoka's formula [9,10], which is applicable to the anchor-type impeller employed in the experiments, was used to determine the power number $N_p$, the power consumption $P$, and the power input per unit reactor volume $P_V$ for the 100 mL and 500 mL reactors. Here, the dimensions of the impellers used in each reactor, as shown in Figures 1 and 2, were employed. Considering that both the power input per unit volume $P_V$ imparted to the fluid by the impeller and the mass of the aluminum alloy $m_{Al}$ are positively correlated with hydrogen production, $P_V \cdot m_{Al}$ was calculated for each reactor. The results are presented in Table 2.

**Table 2.** The power input per unit volume $P_V$, mass of aluminum alloy particle $m_{Al}$, and $P_V \cdot m_{Al}$ in the 100 mL and 500 mL reactors. The power number was calculated using Kamei and Hiraoka's formula [21,22]. Measured hydrogen volume at 72 h were also indicated.

| | | 100 mL Reactor | 500 mL Reactor | 500 mL Reactor |
|---|---|---|---|---|
| Liquid volume $V_L$ (mL) | | 80 | 400 | |
| Power number $N_P$ (-) | | 1.68 | 2.21 | |
| Power $P$ (W) | | 0.12 | 1.30 | |
| Power per volume $P_V$ (W/m$^3$) | | 1513 | 3259 | |
| Mass of aluminum alloy particle $m_{Al}$ (g) | | 5 g | 5 g | 25 g |
| $P_V \cdot m_{Al}$ (W/m$^3$·kg) | | 7.57 | 16.3 | 81.5 |
| Measured hydrogen volume at 72 h (mLstd) | Al–50 wt% Sn | 2008 | 2007 | 12,850 |
| | Al–5 wt% Sn | 1304 | 1081 | 6800–7900 |

As shown in the table, when the alloy mass is 5 g, the $P_V \cdot m_{Al}$ values for the 100 mL and 500 mL reactors are 7.57 and 16.3 W/m$^3$·kg, respectively, with the 500 mL value being approximately twice that of the 100 mL reactor. In contrast, according to the hydrogen generation data in the table, the value for the 500 mL reactor is only about 0.8–1.0 times that for the 100 mL reactor. Meanwhile, when the alloy mass is 25 g in the 500 mL reactor, the $P_V \cdot m_{Al}$ value is 81.5, which is about 11 times that for the 100 mL reactor with an alloy mass of 5 g. In contrast, based on the hydrogen generation data in the table, the value for the 500 mL reactor is approximately 5–6 times that for the 100 mL reactor. These results indicate that, at present, a clear correlation between hydrogen generation and the $P_V \cdot m_{Al}$ value has not been established. In future work, measurements of hydrogen production will be conducted by varying the reactor scale, stirring speed, and mass of aluminum alloy in order to examine these correlations in greater detail.

## 6. Conclusions

In this study, the hydrogen production process based on the stirred aluminum–water reaction without a catalyst and surface activation was experimentally investigated using 100 mL and 500 mL reactors. The results are summarized below:

(1) In the 500 mL reactor, the hydrogen production at 72 h resulting from the reaction of 25 g of Al–50 wt% Sn and Al–5 wt% Sn alloy particles with water was 5 to 6.5 times greater than that obtained in the 100 mL reactor using 5 g of alloy powder, exceeding the scale ratio of the reactors.

(2) For the particles before and after the experiments, surface SEM observations and cross-sectional SEM and EPMA analyses were performed. The results indicated that, in the case of the Al–50 wt% Sn alloy, the reaction proceeded into the particle interiors, which corresponds to the higher hydrogen production compared with the Al–5 wt% Sn alloy.

(3) Hydrogen production exceeding the expected scale ratio is attributed to mechanical energy from the impeller, which enhances alloy particle fragmentation and accelerates the reaction rate. As a means to quantify this effect, the correlation between the product of the alloy powder mass and the impeller power input per unit volume $P_V \cdot m_{Al}$ and the hydrogen production was examined. It was observed that the amount of hydrogen produced tended to increase with $P_V \cdot m_{Al}$; however, a clear correlation has not yet been established.

(4) These results provide preliminary insights into the scale effects necessary for the application of this hydrogen production technology to an actual plant. For realization in practical plants, the demonstration of hydrogen production using large-scale reactors approaching actual plant size remains a future challenge.

**Author Contributions:** Conceptualization, R.I.; methodology, R.N., Y.Y. and M.S.; investigation, R.N., Y.Y. and M.S.; resources, R.I.; writing—original draft preparation, R.N. and Y.Y.; writing—review and editing, R.I.; supervision, R.I. All authors have read and agreed to the published version of the manuscript.

**Funding:** Part of this research was funded by JKA, grant number 2023M-248.

**Institutional Review Board Statement:** Not applicable.

**Informed Consent Statement:** Not applicable.

**Data Availability Statement:** The data presented in this study are available upon request from the corresponding author.

**Conflicts of Interest:** The authors declare no conflicts of interest.

## References

1. Osman, A.I.; Mehta, N.; Elgarahy, A.M.; Hefny, M.; Al-Hinai, A.; Al-Muhtaseb, A.H.; Rooney, D.W. Hydrogen production, storage, utilisation and environmental impacts: A review. *Environ. Chem. Lett.* **2022**, *20*, 153–188. [CrossRef]
2. Wang, H.Z.; Leung, D.Y.C.; Leung, M.K.H.; Ni, M. A review on hydrogen production using aluminum and aluminum alloys. *Renew. Sustain. Energy Rev.* **2009**, *13*, 845–853. [CrossRef]
3. Chang, S.H.; Rajuli, M.F. An overview of pure hydrogen production via electrolysis and hydrolysis. *Int. J. Hydrogen Energy* **2024**, *84*, 521–538. [CrossRef]
4. Huang, X.N.; Lv, C.; Wang, Y.; Shen, H.; Chen, D.; Huang, Y. Hydrogen generation from hydrolysis of aluminum/graphite composites with a core–shell structure. *Int. J. Hydrogen Energy* **2012**, *37*, 7457–7463. [CrossRef]
5. Jia, Y.; Shen, J.; Meng, H.; Dong, Y.; Chai, Y.; Wang, N. Hydrogen generation using a ball-milled Al/Ni/NaCl mixture. *J. Alloys Compd.* **2014**, *588*, 259–264. [CrossRef]
6. Preez, S.P.; Bessarabov, D.G. Hydrogen generation by the hydrolysis of mechanochemically activated aluminum-tin-indium composites in pure water. *Int. J. Hydrogen Energy* **2018**, *43*, 21398–21413. [CrossRef]
7. Xiao, F.; Guo, Y.; Li, J.; Yang, R. Hydrogen generation from hydrolysis of activated aluminum composites in tap water. *Energy* **2018**, *157*, 608–614. [CrossRef]
8. Xiao, F.; Yang, R.; Li, J. Hydrogen generation from hydrolysis of activated aluminum/organic fluoride/bismuth composites with high hydrogen generation rate and good aging resistance in air. *Energy* **2019**, *170*, 159–169. [CrossRef]
9. Zhao, C.; Xu, F.; Sun, L.; Chen, J.; Guo, X.; Yan, E.; Yu, F.; Chu, H.; Peng, H.; Zou, Y.J.; et al. A novel Alsingle bondBiOCl composite for hydrogen generation from water. *Int. J. Hydrogen Energy* **2019**, *44*, 6655–6662. [CrossRef]
10. Guan, X.; Zhou, Z.; Luo, P.; Wu, F.; Dong, S. Hydrogen generation from the reaction of Al-based composites activated by low-melting-point metals/oxides/salts with water. *Energy* **2019**, *188*, 116107. [CrossRef]
11. Manilevich, F.D.; Pirskyy, Y.K.; Kutsyi, A.V.; Berezovets, V.V.; Yartys, V.A. Aluminium as an efficient energy storage substance for the catalysed generation of hydrogen from water. *J. Energy Storage* **2014**, *96*, 112748. [CrossRef]
12. Sevastyanova, L.G.; Klyamkin, S.N.; Stupnikov, V.A.; Ilyukhina, A.V.; Bulychev, B.M. On mechanism of hydrogen generation at oxidation of activated aluminum in aqueous solutions. *Int. J. Hydrogen Energy* **2024**, *54*, 428–436. [CrossRef]
13. Gai, W.-H.; Zhang, X.; Sun, K.; Deng, Z. Hydrogen generation from Al-Water reaction promoted by M-B/γ-Al2O3 (M = Co, Ni) catalyst. *Int. J. Hydrogen Energy* **2019**, *44*, 24377–24386. [CrossRef]
14. Prabu, S.; Wang, H.W. Enhanced hydrogen generation from graphite-mixed aluminum hydroxides catalyzed Al/water reaction. *Int. J. Hydrogen Energy* **2020**, *45*, 33419–33429. [CrossRef]
15. Chen, Y.-T.; Huang, L.-Y.; Wang, H.W. Optimization of aluminum hydroxide catalyst for efficient hydrogen generation from aluminum-water reaction. *Int. J. Hydrogen Energy* **2024**, *91*, 303–309. [CrossRef]
16. Teng, H.-T.; Lee, T.-Y.; Chen, Y.-K.; Wang, H.W.; Cao, G. Effect of Al(OH)3 on the hydrogen generation of aluminum–water system. *J. Power Sources* **2012**, *219*, 16–21. [CrossRef]
17. Kanda, Y.; Kondo, S.; Ooya, S.; Kobayashi, T.; Uemichi, Y.; Higashino, K.; Sugioka, M. Green Hydrogen Production by Mechanical Mixing of Aluminum with Water. *J. Chem. Eng. Jpn.* **2011**, *44*, 803–808. [CrossRef]

18. Sugioka, M.; Higashino, K.; Uemichi, Y.; Kanda, Y. Production of Green Hydrogen by Mechanical Mixing of Aluminum with Water using Stainless Steel Reactor. In Proceedings of the 14th Asia Pacific Confederation of Chemical Engineering Congress, Singapore, 21–24 February 2012.
19. Nishiyama, R.; Imai, R. Study of hydrogen production method by reaction of Al powder and water with Stirling (Discussion about time history of hydrogen production rate). In Proceedings of the 26th The National Symposium on Power and Energy Systems, Saga, Japan, 13–14 July 2022. (In Japanese)
20. Nishiyama, R.; Imai, R. Study of hydrogen production method by reaction of Al alloy powder and water with stirring (Effect of Al alloy powder concentration on reaction). In Proceedings of the 27th The National Symposium on Power and Energy Systems, Tokyo, Japan, 20–21 September 2023. (In Japanese)
21. Furukawa, H.; Kato, Y.; Inoue, Y.; Kato, T.; Tada, Y.; Hashimoto, S. Correlation of Power Consumption for Several Kinds of Mixing Impellers. *Int. J. Chem. Eng.* **2012**, *2012*, 106496. [CrossRef]
22. Kamei, N.; Hiraoka, S.; Kato, Y.; Tada, Y.; Shida, H.; Lee, Y.S.; Yamaguchi, T.; Koh, S.T. Power correlation for paddle impellers in spherical and cylindrical agitated vessels. *Kagaku Kogaku Ronbunshu* **1995**, *21*, 41–48. [CrossRef]

**Disclaimer/Publisher's Note:** The statements, opinions and data contained in all publications are solely those of the individual author(s) and contributor(s) and not of MDPI and/or the editor(s). MDPI and/or the editor(s) disclaim responsibility for any injury to people or property resulting from any ideas, methods, instructions or products referred to in the content.